

Influence of water vapor and aerosols on downward longwave radiation in the high mountain region of Musala peak, Bulgaria

Peter Nojarov ^{a,*} , Todor Arsov ^b , Ivo Kalapov ^b , Hristo Angelov ^b 

^a National Institute of Geophysics, Geodesy and Geography, Bulgarian Academy of Sciences, Sofia, Bulgaria

^b Institute of Nuclear Research and Nuclear Energy, Bulgarian Academy of Sciences, Sofia, Bulgaria

*Corresponding author: pnojarov@abv.bg

Key words:

aerosols, Bulgaria, downward longwave radiation, high mountain, water vapor

ABSTRACT

This study reveals the effect of aerosols and water vapor on downward longwave radiation in the high mountain region of Musala peak, Bulgaria. The investigated period is 01/01/2017 (Jan. 1st 2017) – 30/09/2019 (Sep. 30th 2019). Statistical methods are the main tool for discovering the relationships between the different elements. The results indicate that air temperature is the leading factor for downward longwave radiation, specific humidity, and amount of aerosols in the air. That is why, in order to reveal the pure relationship between downward longwave radiation, specific humidity and amount of aerosols in the atmosphere, the air temperature was cleared from the data series. After this procedure, the results show that specific humidity has a significant influence on the downward longwave radiation flux, and an increase of 1% of the specific humidity results in an increase of about 12-15% in the values of the downward longwave radiation. At air temperatures around 0°C the influence of water vapor on the downward longwave flux is highest, which is due to the phase transitions of the water – a process during which release/absorption of radiation in the longwave spectrum occurs. The amount of aerosols in the atmosphere also has a significant effect on this type of radiation, and an increase of 1% of the amount of aerosols in the air at air temperatures above –5.5°C results in an increase of the downward longwave radiation of about 2-4%. The findings of this study show that coarser and opaque aerosol particles have a stronger effect on downward longwave radiation. In the area of Musala peak, as the air temperature rises, there is an increase in the amount of aerosols in the air, a decrease in their size, and a transition from transparent to opaque aerosols. The combination of these different tendencies causes the influence of aerosols on downward longwave radiation to be strongest in the middle temperature interval – air temperatures between –5.5°C and +5.5°C. Due to the increased total amount of aerosols and increased amount of opaque aerosols, their influence on downward longwave radiation is significant also at air temperatures above 5.5°C.

Article processing

Submitted: 01 September 2021

Accepted: 13 October 2021

Published: 01 November 2021

Academic editor: Mariyana Nikolova

© P. Nojarov et al. This is an open access article distributed under the terms of the Creative Commons Attribution License (CC BY 4.0), which permits unrestricted use, distribution, and reproduction in any medium, provided the original author and source are credited.

1. Introduction

In the last century, warming has been one of the major processes taking place in the Earth's atmosphere, and in particular – the troposphere, which is the layer closest to the Earth's surface. The main reason for this is the change in the troposphere's gas composition through increasing of the so-called greenhouse gases such as water vapor, carbon dioxide, methane, etc. The mechanism which causes this warming is that these greenhouse gases absorb longwave radiation (wavelengths between 3 – 100 μm) emitted from the Earth's surface and return it back to the Earth's surface. In this way, the near surface atmosphere increases its temperature. Therefore, it is of particular importance to monitor and measure not only the quantities of greenhouse gases but also the longwave radiation directed towards the Earth's surface. Also, in recent years, increasing attention has been paid to aerosols and their role in the climate system as a factor for redistribution of radiation fluxes in the



atmosphere. Aerosols are solid or liquid particles suspended in the air. They are of natural or anthropogenic origin and have different sizes and shapes. They also have different chemical composition. These characteristics affect the different radiation fluxes in the atmosphere in various ways, which makes it difficult to model their impact on the atmosphere and their contribution to the warming/cooling of the atmosphere, and in particular – of the troposphere. Thus, studies on aerosols' impact, especially on longwave radiation fluxes, are important. The significance of this type of studies is also determined by the fact that those studies are relatively rare worldwide.

Two types of studies can be distinguished in the literature regarding the effect of aerosols on downward longwave radiation. The first type covers a longer period of time and evaluates the effect regarding that period. Song et al. (2018) evaluate the direct radiative effect of mineral dust in both shortwave (wavelengths between 0.2 – 3 μm) and longwave spectra at the top of the atmosphere and at the Earth's surface. The study concerns the tropical North Atlantic and the main conclusions are that mineral dust has positive radiative effects in the longwave spectrum at both studied atmospheric levels. Wang et al. (2004) studied the radiative effect of dust in the shortwave and longwave spectra in the East Asian and the North Pacific region. They also concluded that dust has a positive radiative effect in the longwave spectrum, both at the Earth's surface and at the top of the atmosphere. Similar conclusions are drawn in the paper by Wang et al. (2017), who also studied dust, concluding that the greater its amount in the atmosphere is, the greater its positive radiative effect in the longwave spectrum is. The importance of water vapor in such type of effect assessment is emphasized. The positive radiative effect in the longwave spectrum of aerosols at various locations around the world is also revealed in the works of Panicker et al. (2008), and Maghrabi et al. (2019).

The other type of studies refer to a specific event, usually a heavy dust event, that affects a specific location for a limited period of time – within a few days. During this event, measurements of the downward longwave radiation, as well as the content and other characteristics of aerosols in the atmosphere, are made. The works of Maghrabi and Al-Dosari (2016), Barragan et al. (2016), and Antón et al. (2014), are of this type. All three studies show a significant increase of the downward longwave radiation at the Earth's surface when a particular event occurs. That increase ranges from 3.5–20 $\text{W}\cdot\text{m}^{-2}$ for locations in the Mediterranean to 41 $\text{W}\cdot\text{m}^{-2}$ for locations in the Arabian Peninsula. In general, in all these studies, particular attention is paid to dust, which is a solid aerosol and has a relatively large particle size. For this reason, dust also absorbs some of the shortwave radiation, heats and starts emitting radiation in the longwave spectrum, increasing the amount of longwave radiation directed towards the Earth's surface. This mechanism is typical for dust, but there is still no clarity on the mechanisms that are present in an environment with prevalence of other types of aerosols, as is the case in high mountains.

The aim of this study is to reveal the effect of aerosols and water vapor on the longwave radiation directed towards the Earth's surface for the period between 01/01/2017 and 30/09/2019 in the region of Musala peak, Bulgaria. This location is characterized by specific environmental conditions, which determine a specific interaction between the studied elements. In order to accomplish the aim of the study, the relationships between air temperature, downward longwave radiation flux, specific humidity and total aerosol content, were measured through several parameters. The Angstrom parameter and the absorption and scattering of radiation by aerosols are revealed. On the basis of the established relationships, an attempt is made to

show, as clear as possible, the “sole” effect of aerosols and water vapor on downward longwave radiation. A quantitative assessment of this effect is then made.

2. Instruments, data and methods

“Musala” Basic Environmental Observatory (BEO) Station (Institute of Nuclear Research and Nuclear Energy – Bulgarian Academy of Sciences) is located at Musala peak, Rila Mountain, Bulgaria, at an altitude of 2925 m, with coordinates: 42°11' N and 23°35' E (Figure 1). The station carries out a wide range of environmental parameters' measurements in high mountain conditions, where during most of the year air temperatures are low and there is a constant snow cover. Measurements of downward longwave radiation began in the very end of 2016, which is why the study period of this study is from 01/01/2017 to 30/09/2019.

Downward longwave radiation is measured at “Musala” BEO Station using Kipp and Zonen CGR4 pyrgeometer. The pyrgeometer was installed in the end of 2016 and has been continuously operating since the beginning of 2017. As the pyrgeometer is further equipped with a fan, this reduces the dome heating offset to a negligible level, eliminating the need for dome temperature measurements or dome shading, and in addition to that, the accumulation of snow and ice on the glass dome of the instrument is reduced, which is particularly important in climatic conditions at such altitudes. The pyrgeometer performs measurements every minute in the wavelength range from 4.5 to 42 μm . The pyrgeometer can operate at temperatures from –40 to +80°C – a range that completely covers usual air temperatures at Musala peak.

The meteorological parameters at Musala peak are measured by the “Vaisala” weather station at 2 m above ground. The study uses data for air temperature, relative humidity, atmospheric pressure and specific humidity. The meteorological station's measurements are taken every 10 minutes, while only those measurements that match the time of measurement of the MICROTOPS instrument were selected. During the 2017 – 2019 period, the instrument had no interruptions in its work and thus it does not limit the number of cases used in this study.

The instrument for measurement of aerosol concentration is the TROPOS Scanning Mobility Particle Sizer (TROPOS-SMPS) Spectrometer (Leibniz Institute for Tropospheric Research). The parameter which is measured is particle number concentration. The unit of measurement is dN/dlogDp (cm^{-3}). It shows the number density (concentration) distribution function – the number of particles per volume of air, of a size between D_p and dD_p . Aerosol particle concentration data are collected over an interval of 5 minutes and include a total of 71 particle diameters from 10 nm to 881 nm. In this way the total amount of aerosol particles of all diameters can be calculated. The sum of aerosol particles larger than 285 nm in diameter was also calculated, so as to be able to reveal only the effects of larger aerosol particles on the downward longwave radiation, as well as for other calculations. Due to various technical issues, the SMPS instrument did not work during almost all of 2017, and for about one month from mid-February to mid-March, 2019. This reduces the number of selected cases with measurements of this element to 79, which however, is still sufficient for statistical analysis.

Aerosol Optical Thickness (AOT) measurements at 1020 nm were performed using the Solar Light MICROTOPS II Ozone Monitor and Sunphotometer. Measurements are made manually by the observer at the station in cloudy or fog-free conditions approximately every hour during the day. There were no technical problems with

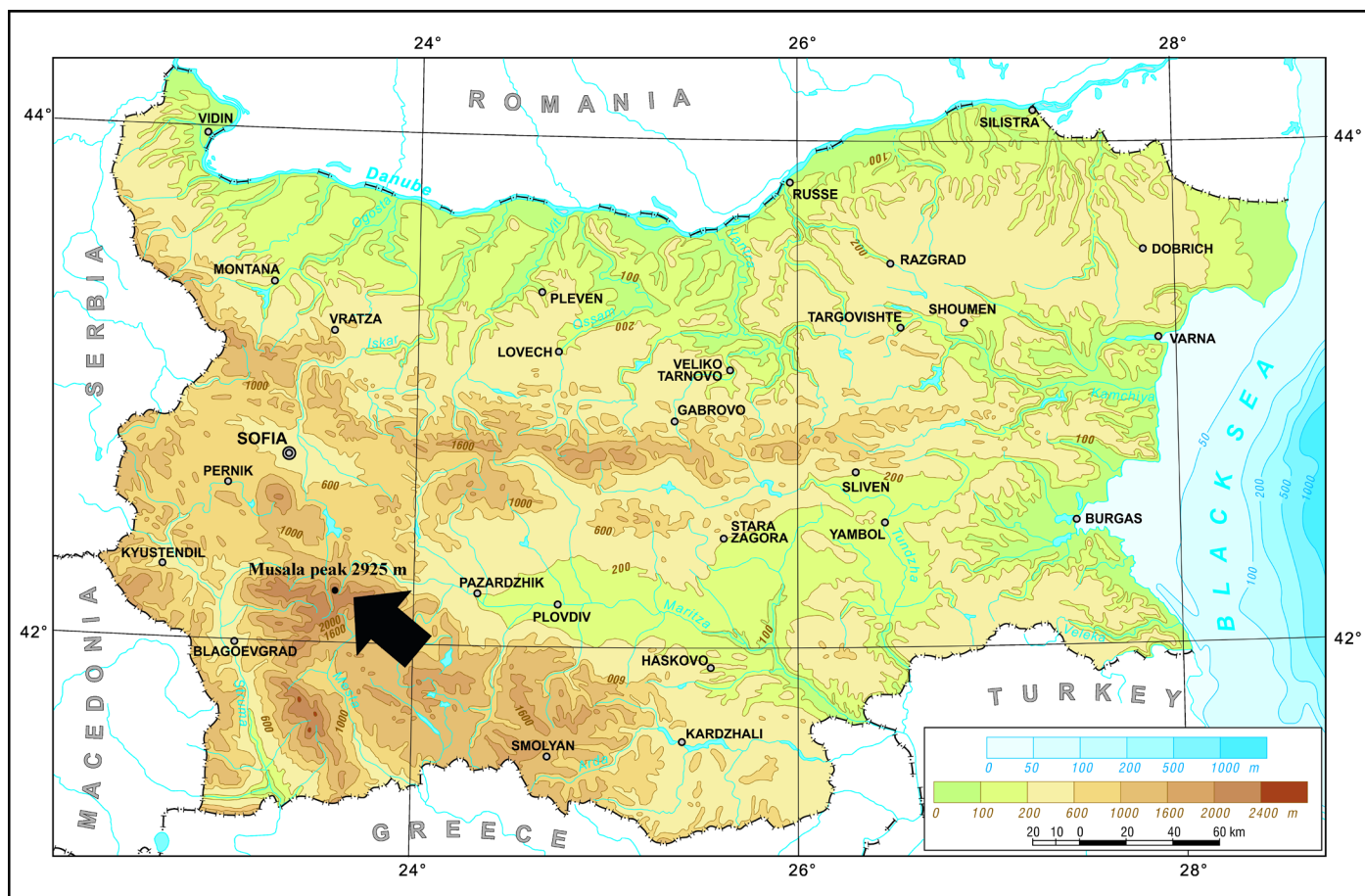


Figure 1. Location of Musala peak within the territory of Bulgaria and in relation to the neighbouring countries.

this device during the studied period. However, some outliers were removed from the dataset and therefore the total number of cases is 147. The outliers were determined by comparison with data from other devices measuring aerosol concentration, as well as with the data from MERRA-2 reanalysis. As the temporal measurement frequency here is lowest (1 hour), these data became reference data in terms of specific hour and minute, while the data from other instruments (which have a higher measurement frequency) were selected to match those hours and minutes.

In order to avoid the significant effect of clouds on downward longwave radiation, only cases with cloud-free sky during the studied period were selected. Measurements of the aerosol optical thickness at Musala peak with the MICROTOPS instrument were performed only in cloud-free conditions (a passive sensor was used), so they were the prime criterion for the selection of the cases used in the study, which has led to a choice of cases only during the day. The selection of cases was supported also by the data from the nearby meteorological station of the National Institute of Meteorology and Hydrology, which is synoptic, and reports on a 3-hour basis, including observations on cloudiness. The data from the pyranometer (Kipp and Zonen CMP10) which measures the global shortwave solar radiation at “Musala” BEO were also reviewed, where the presence of clouds is easily detected by a sharp (more than 1% per minute) decrease in the measured values. Due to the distinct daily course of the cloudiness at Musala peak (especially in the warm half-year),

with an afternoon maximum, the selected cases are from the first half of the day, but close to noon, so that the Sun could be high above the horizon. All this led to a selection of cases from 10.30 to 12.30 local time, under cloud-free conditions.

Aerosol data from The Modern-Era Retrospective Analysis for Research and Applications, Version 2 (MERRA-2) (Gelaro et al., 2017) were also used. This reanalysis has a horizontal resolution of $0.5^\circ \times 0.625^\circ$ latitude \times longitude, and a vertical resolution of 72 layers, reaching approximately 85 km of altitude. Aerosol data are based mainly on the MODIS (Moderate Resolution Imaging Spectroradiometer) instrument, Terra and Aqua satellites. Both satellites are in Sun-synchronous orbit, with Terra satellite passing over a certain location at about 10.30 local time, and Aqua – at about 13.30 local time. Thus, their measurements largely coincide with those of the ground-based instruments. Aerosols data from MERRA-2 reanalysis used here are the Ångström parameter 470-870 nm, and AOT at 550 nm. The grid-cell which covers Musala peak has the following coordinates: 42-42.5°N and 23.125-23.75°E. There are data for the entire studied period.

Measurements of the absorption of radiation by aerosols are performed using the NOAA Continuous Light Absorption Photometer (CLAP). It measures the absorption of radiation at three wavelengths – blue (467 nm), green (529 nm) and red (653 nm). The measurements here are taken every minute. The device started its operation on 23/04/2017 and there have been some interruptions

due to technical issues in the subsequent period, which reduces the number of cases, but it does not fall below 84 cases and is, therefore, sufficient for statistical analysis. Usually, in climatology a sample size of 30 or more numbers is considered good for statistical analysis.

Measurements of scattering coefficients at three spectra – blue (450 nm), green (550 nm) and red (700 nm) were carried out using the TSI3563 Nephelometer. Data are collected every minute. The angles of measurement of scattering are between 7 and 170°. The study of Dufresne et al. (2002) discusses the effect of aerosol scattering on the radiative effect in the longwave spectrum. The conclusions indicate that this effect becomes significant and should be considered for particles with a diameter larger than 1000 nm. Figure 2 shows the distribution of aerosols by particle diameter for the selected cloud-free cases during the studied period. Aerosols with a particle size of up to about 100 nm (with a peak at about 17 nm) predominate at Musala peak. Distribution of aerosols of such size, with a predominance of the fine mode, is characteristic also for other high mountain stations (Venzac et al. 2008; Weingartner et al. 1999). On the other hand, the scattering in the shortwave spectrum is directly proportional to the total amount of aerosols at a given place. This means that scattering can be used to quantify the amount and size of aerosols in the air. In order to estimate the dominating aerosol particle size and to characterize the haziness of the atmosphere, scatter-related Angstrom exponents are used (Del Guasta and Marini, 2000; Del Guasta, 2002). They are an analog of the classical extinction-related Angstrom exponents (Angstrom, 1964), derived from a version of the Angstrom law, as expressed in terms of scattering coefficients, when using two wavelength nephelometer data. Similarly to the classical Angstrom exponents, scatter-related Angstrom exponents are nearly wavelength-independent in wide spectral domains. At the same time, they are sensitive to the aerosol particle size distribution. In this study the classical Angstrom formula was used to calculate α (Angstrom exponent) and β (turbidity coefficient), where aerosol optical thickness was replaced with scattering coefficients. Angstrom exponents for one couple (450-700 nm, blue-red) of wavelengths were calculated.

The data in Figure 2, as well as the data presented in the study of Asmi et al. (2011) show that the aerosol content in the area of Musala peak is higher compared to other similar mountain stations (Zugspitze 2650 m, Jungfrauoch 3580 m, Monte Cimone 2165 m). The aerosol content at Musala peak is also higher than that at some low-lying stations in northern Europe (Aspvreten – 30 m, Birkenes

– 190 m, Pallas – 560 m). Given that the water vapor content in the atmosphere at an altitude of approximately 3000 m is relatively low, the area of Musala peak is particularly suitable for studying the effect of aerosols on downward longwave radiation.

The specific humidity at Musala peak was calculated on the basis of data for air temperature, relative humidity and atmospheric pressure. The following formulas were used in the calculations:

$$s = 0.622 \cdot \frac{e}{p} \quad (1)$$

where s is the specific humidity ($\text{kg} \cdot \text{kg}^{-1}$), e is the water vapor pressure and p is the atmospheric pressure; e can be calculated using the following formula:

$$e = r \cdot e_s \quad (2)$$

where r is the relative humidity and e_s is the water vapor saturation pressure, which is a function of temperature T . The relationship between T and e_s is given by the following formula (Magnus equation with respect to water, Donev 1983):

$$e_s = e_0 \cdot 10^{\frac{7.45 \cdot T}{235 + T}} \quad (3)$$

where T is the air temperature in °C and e_0 is the water vapor saturation pressure at temperature 0°C.

Various methods were used in the statistical analysis (Wilks 2006). Statistically significant results are those, where the significance level is $p < 0.05$. The statistical distribution of the data series was determined in order to see whether linear methods could be applied or not. Chi-square statistic was used to estimate the degree of fitting to a certain distribution. The smallest value of this statistic indicates the best fit to a certain distribution. The statistical distribution of downward longwave radiation and specific humidity is normal. However, the distribution of the other variables is, in most cases, different from normal (e.g. AOT_{1020} , AOT_{550} , etc.). That is why the nonparametric Spearman's rank correlation was used in this study, in which the distribution does not influence the final result. In this way, the relationships between the studied variables were revealed. These relationships are described by linear, as well as by nonlinear models. The linear model equation is as follows:

$$y = a + b \cdot x \quad (4)$$

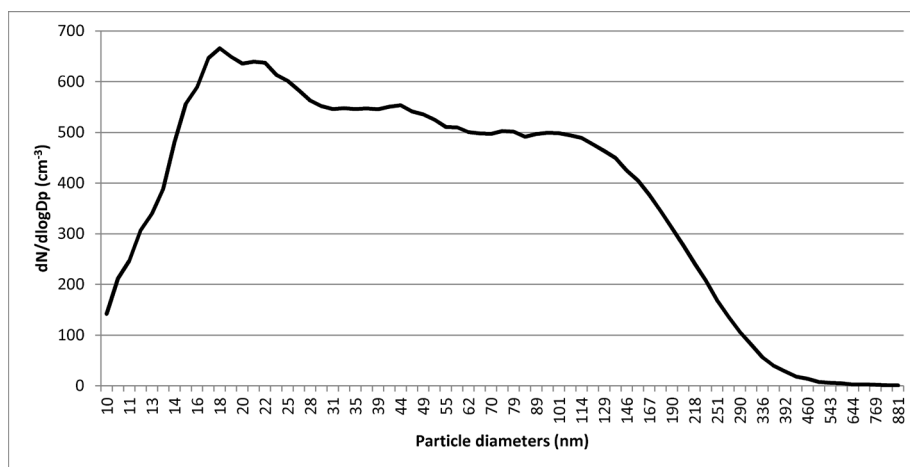


Figure 2. Distribution of aerosols by particle size (diameters in nm) for the period 01/2017 – 09/2019 at “Musala” BEO station. Y-axis represents the mean amount of aerosols (in dN/dlogD_p , cm^{-3}) from all 160 cases under clear sky conditions (adapted from: Nojarov et al. 2021).

where a and b are coefficients, x is the independent variable and y is the dependent variable

The nonlinear model is an S-curve type and its equation is as follows:

$$y = e^{c + \left(\frac{d}{x}\right)} \quad (5)$$

where, c and d are coefficients, x is the independent variable and y is the dependent variable.

The way of calculating the percentage change in the dependent variable as a function of the change in the independent variable will be presented later in the text.

3. Results and discussion

Air temperature is an important factor for both the amount of downward longwave radiation and other studied elements. Figure 3 shows the variations of air temperature and downward longwave radiation for the selected cases during the period 01/2017 – 09/2019. It can be seen that the two indicators are fully synchronized, with a summer maximum and a winter minimum. This is also confirmed by the results in Table 1, which show the correlation coefficients (Spearman's correlation) between air temperature and other studied elements. The correlation between air temperature and downward longwave radiation is positive and statistically significant, and has a very high value. The cause for the observed close relationship is that air temperature practically measures the flux of longwave radiation emitted from the Earth's surface. This flux is the main income part for the heating of near surface air and all the gases and aerosols contained therein, which then emits radiation also in the longwave spectrum. Part of this radiation is directed back to the Earth's surface, and in fact, this is the measured downward longwave radiation. In this way, the greenhouse effect is realized. In a previous study (Nojarov, 2017), which covers the entire territory of Bulgaria, and is based on weather station air temperature measurements and

ERA-Interim reanalysis data for the downward longwave radiation flux, a lower positive value of correlation between these two elements was obtained, but it is still statistically significant. The cause for this difference is that in the previous study the cases with cloud cover were not excluded, and cloud cover has a significant influence on downward longwave radiation.

Table 1. Spearman's correlation coefficients between air temperature and the other studied variables for the period 01/2017-09/2019 at Musala peak. Statistically significant coefficients are bolded.

	Air temperature
Downward longwave radiation	0.93
Specific humidity	0.74
AOT ₁₀₂₀	0.51
AOT ₅₅₀	0.32
SMPS _{totalsum}	0.57
SMPS _{sum>285}	0.66
Angstrom parameter ₄₇₀₋₈₇₀	0.11
Absorption _{blue}	0.46
Absorption _{green}	0.38
Absorption _{red}	0.48
Scattering _{blue}	0.59
Scattering _{green}	0.61
Scattering _{red}	0.55
α Blue-Red scattering coefficient	0.13
β Blue-Red scattering coefficient	0.46

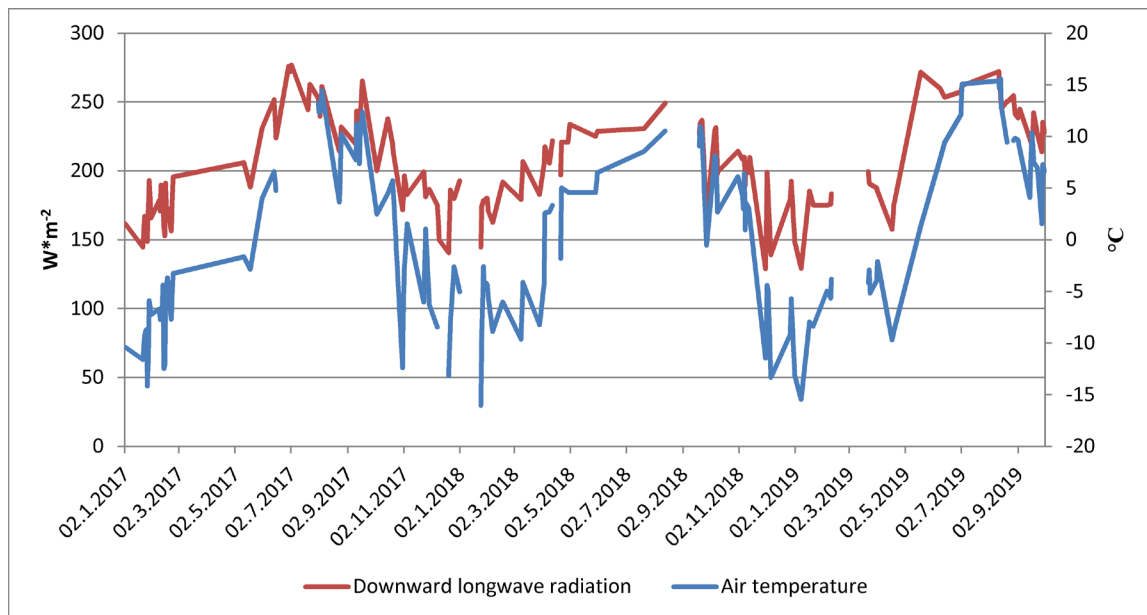


Figure 3. Variations of air temperature (°C) and downward longwave radiation (W*m⁻²) for the selected cases in the period 01/2017 – 09/2019 at Musala peak.

Figure 4 shows the variations of air temperature and specific humidity at Musala peak for the selected cases during the studied period. Here too, a good synchronicity of the curves is observed. This is also confirmed by the correlation coefficient in Table 1, which is positive and statistically significant. The observed dependence is due to the fact that warmer air is able to contain larger amounts of water vapor and vice versa. This is also evident from the formula presented above which describes the connection between water vapor saturation pressure and air temperature. The course of both elements has a summer maximum (highest air temperature) and a winter minimum (lowest air temperature).

Figure 5 shows the variations of air temperature and AOT_{1020} at Musala peak for the selected cases during the studied period. Here too, there is a synchronicity of the curves with a summer maximum and a winter minimum. This strong positive correlation is also evident from the results in Table 1. All studied parameters

representing aerosol content in the air (AOT_{1020} , AOT_{550} , total sum, sum > 285 nm and turbidity coefficient β) have statistically significant positive correlation coefficients. The higher values are typical for the parameters measured directly at “Musala” BEO station, which should be expected given that the air temperature is also measured there. There are basically two causes for the observed significant positive correlation: the first one is that at higher air temperatures upward movements in the atmosphere, as well as the turbulence, increase. The main source of aerosols is the Earth’s surface, and such movements favor their propagation into the atmosphere in general, and into its higher layers in particular. The second cause is the type of surface in the region of Musala peak – in winter, at lower air temperatures, the Earth’s surface is covered with snow, which prevents aerosols (especially dust) from entering the atmosphere. In summer, such cover is not present and, accordingly, aerosols from the Earth’s surface have free access to the atmosphere.

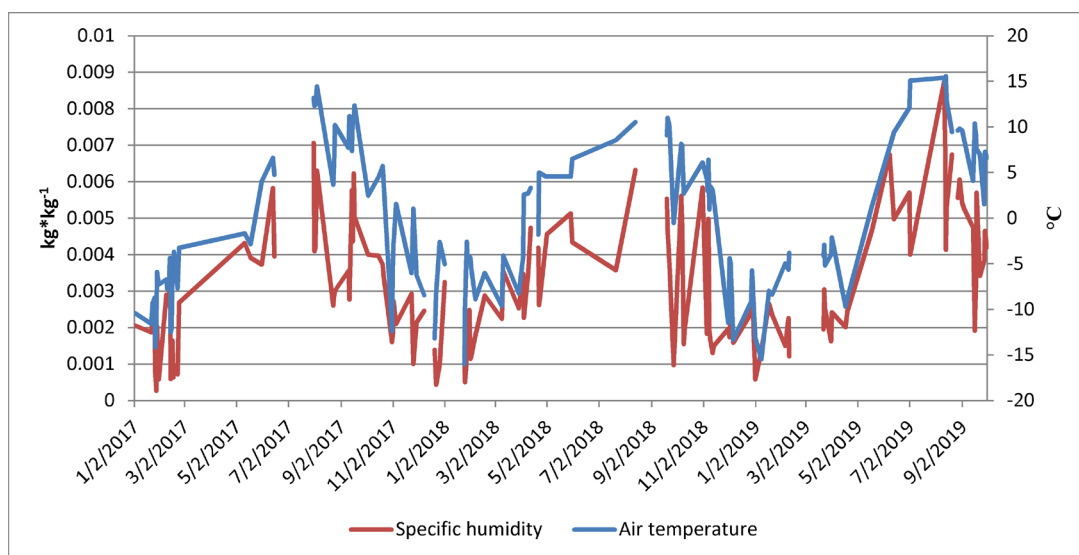


Figure 4. Variations of air temperature (°C) and specific humidity ($\text{kg} \cdot \text{kg}^{-1}$) for the selected cases in the period 01/2017 – 09/2019 at Musala peak.

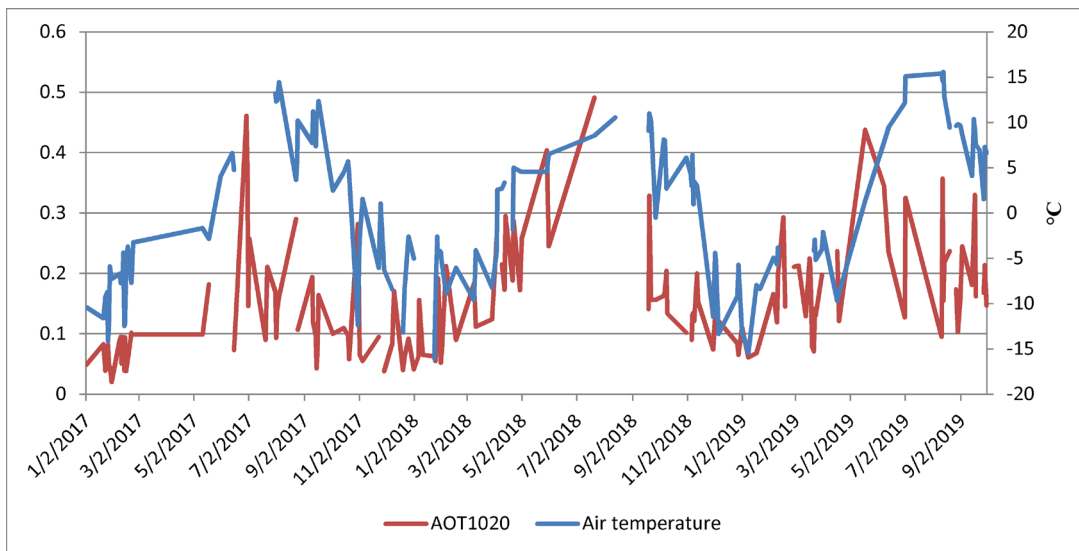


Figure 5. Variations of air temperature (°C) and AOT_{1020} for the selected cases in the period 01/2017 – 09/2019 at Musala peak.

Another potential effect of air temperature on the amount of aerosols at Musala peak should be noted, and it is not of a cause-effect type. In the study of Nojarov et al. (2014), it was revealed that air transport from, generally the northern quarter of the horizon, leads to a significant increase in the total amount of aerosols at Musala peak and vice versa. However, in Bulgaria, the air coming from this direction usually has lower temperatures than that coming from the southern quarter of the horizon. In this way, only due to the influence of the atmospheric circulation and advection of the respective type of air, an inverse relationship is created between the amount of aerosols and the air temperature, i.e. lower temperatures will be associated with higher amounts of aerosols and vice versa. Thus, this dependence is not direct but is mediated through a third element.

A number of studies (Angstrom, 1918; Brunt, 1932; Swinbank, 1963; Idso and Jackson, 1969; Brutsaert, 1975; Prata, 1996) have developed mathematical models for calculating downward longwave radiation in different geographical locations. These models are based on data for two main elements – air temperature and water vapor content, expressed by its pressure. Those studies follow the theory that these two elements are very closely related to the downward longwave radiation.

All of the above shows the great influence of air temperature on the other studied elements. If it is necessary to investigate the pure relationships between, for example, downward longwave radiation and the amount of aerosols in the atmosphere, this factor should be removed from the initial data. In the present study, this is done as follows: the data used in this study were divided into three groups depending on air temperature. In the area of Musala peak, it ranges from approximately -16°C to $+16^{\circ}\text{C}$ for the selected cases. Three groups of data that have the same temperature interval of 11°C were created:

- cases with air temperature below -5.5°C ;
- cases with air temperature between -5.5°C and $+5.5^{\circ}\text{C}$;
- cases with air temperature above $+5.5^{\circ}\text{C}$.

In this way, the seasonality of the studied elements (downward longwave radiation, specific humidity and aerosol content in the air), which is due to the temperature factor, is largely cleared. On the other hand, the impact that (for example) specific humidity (water vapor) has on air temperature through the process of returning of longwave radiation to the Earth's surface, are kept. This allows a more accurate and complete investigation of the existing relationships between the studied variables.

Referring again to Table 1, it can be seen that both Angstrom parameters (MERRA-2 and nephelometer) have a statistically insignificant correlation with air temperature. Absorption and scattering at the three wavelengths (blue, green and red) have a statistically significant positive correlation with air temperature. However, it should be borne in mind that due to the way of measurement of the instruments, the absorption and scattering are directly related to the amount of aerosols, i.e. more aerosols will lead to more absorption and scattering, and vice versa. This affects the correlation coefficient values shown in Table 1. The above is illustrated by the variations of AOT_{550} and absorption_{green} for the selected cases in the study period, which are shown in Figure 6. It can be seen that they are synchronous with a summer maximum and a winter minimum. These results confirm that the correlation with air temperature in Table 1 is not direct but depends on the amount of aerosols.

Table 2 shows the statistical distribution and the respective Chi-square value of the different studied elements for the three air temperature intervals. The table reveals that the downward longwave radiation, the specific humidity and both Angstrom parameters have a normal distribution in all air temperature intervals. The other variables (various indicators for the amount of aerosols in the atmosphere, as well as the absorption and scattering of radiation at the three wavelengths) have either gamma distribution or log-normal distribution. This justifies the need to use Spearman's correlation, as well as a nonlinear model of relationship between two variables, as explained in the Instruments, Data and Methods section of the paper.

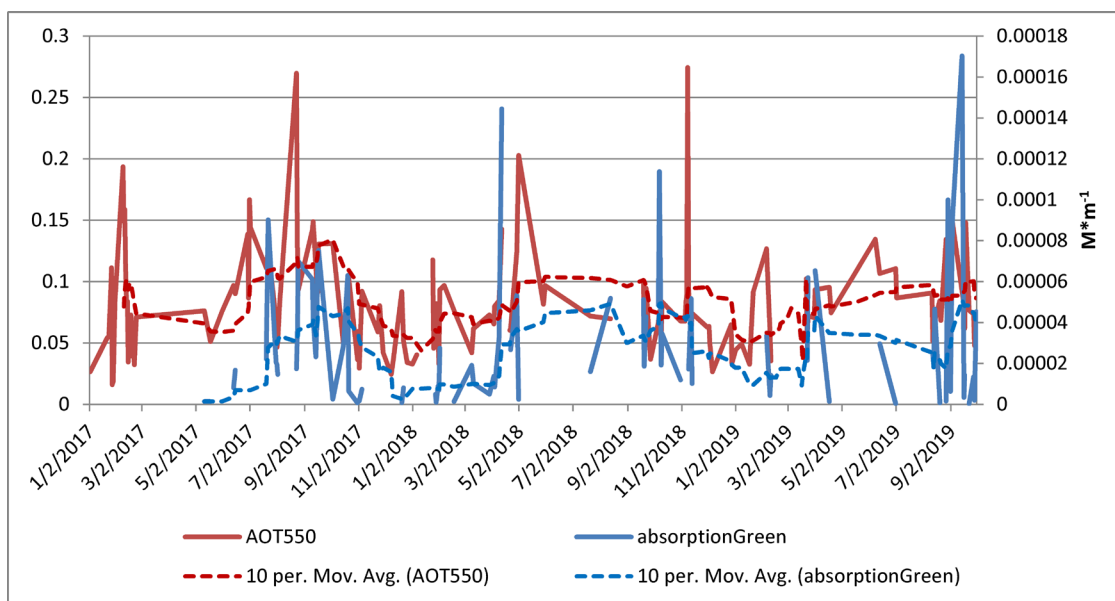


Figure 6. Variations of AOT_{550} and absorption_{green} (M^*m^{-1}) for the selected cases in the period 01/2017 – 09/2019 at Musala peak (10 cases' moving averages of the two variables are also shown in the figure).

Table 2. The best fitting statistical distribution and the respective Chi-square value of the studied variables at Musala peak for the different air temperature intervals during the period 01/2017 – 09/2019.

Variable	Air temperature below -5.5°C		Air temperature between -5.5°C and +5.5°C		Air temperature above 5.5°C	
	Distribution	Chi-square value	Distribution	Chi-square value	Distribution	Chi-square value
Downward longwave radiation	Normal	4.9	Normal	2.3	Normal	2
Specific humidity	Normal	5.5	Normal	6.6	Normal	0.2
AOT ₁₀₂₀	Log-normal	1.7	Log-normal	4	Log-normal	1.2
AOT ₅₅₀	Log-normal	0.8	Gamma	5.8	Gamma	2.5
SMPS _{totalsum}	Log-normal	17.5	Log-normal	51.2	Gamma	0.4
SMPS _{sum>285}	Gamma	17.9	Gamma	19.7	Log-normal	9.1
Angstrom parameter ₄₇₀₋₈₇₀	Normal	6.1	Normal	10.8	Normal	8.3
Absorption _{blue}	Gamma	9.1	Log-normal	11.4	Gamma	1.9
Absorption _{green}	Gamma	11.1	Log-normal	9.3	Gamma	3.1
Absorption _{red}	Gamma	20.4	Log-normal	2.4	Gamma	0.1
Scattering _{blue}	Log-normal	16.4	Gamma	0.2	Gamma	8.2
Scattering _{green}	Log-normal	34.6	Gamma	5.2	Gamma	5.6
Scattering _{red}	Log-normal	23.1	Log-normal	1.1	Gamma	3.4
α Blue-Red scattering coefficient	Normal	2.6	Normal	17.1	Normal	6.8
β Blue-Red scattering coefficient	Gamma	26.3	Log-normal	10.4	Gamma	3.1

The calculated Spearman's correlation coefficients for the three air temperature intervals are shown in Table 3. In all three air temperature intervals the specific humidity is in a positive and statistically significant relationship with the downward longwave radiation. This proves the significant influence of water vapor even in the absence of clouds. Another thing that has to be pointed out is that the correlation coefficient is highest in the temperature interval from -5.5°C to $+5.5^{\circ}\text{C}$. These are the temperatures around 0°C , at which a phase transition between the liquid and the solid state of water takes place. During this phase transition, heat in the longwave radiation spectrum is released/absorbed. This mechanism enhances the influence of water vapor on downward longwave radiation at air temperatures around 0°C . When investigating the relationship between aerosols and downward longwave radiation, several characteristics of aerosols must be considered: the first one is their total amount, which can be in the near-surface layer of air or in the entire atmosphere column above a given point. The amount of aerosols in the near-surface air layer is measured by the TROPOS-SMPS and the nephelometer (turbidity coefficient) instruments, and the amount in the entire air column – by the MICROTOPS instrument and the MERRA-2 reanalysis. The second characteristic is the size of aerosols, expressed by the Angstrom parameters. The third characteristic is the type of aerosols. The amount of aerosols in the near-surface layer of air (according to the data from both instruments) increases with increasing air temperature, i.e. in the temperature interval below -5.5°C it is the lowest, while in the following intervals it gradually increases. The same distribution by temperature intervals is observed for the amount of aerosols in

the entire atmosphere column above Musala peak (AOT data). In terms of aerosol particle size, both Angstrom parameters show an increase in their values with the increase of air temperature. This means that at lower air temperatures, coarser aerosols predominate and vice versa. The study of Nojarov et al. (2014) has revealed that transparent or translucent aerosols predominate at Musala peak. The above facts show that in the interval with the lowest air temperatures (below -5.5°C) there is a lower amount of aerosols, which however, are coarser and more transparent. This means that aerosols are probably (during the cold part of the year) snow or ice particles. At temperatures above 5.5°C the aerosols are higher in quantity but finer in size and, given the lack of snow cover, are probably of an opaque type such as dust. In general, the higher the amount of aerosols is in the air, the stronger their effect on downward longwave radiation should be. However, Table 3 shows that this is not the case. All studied variables that measure the concentration of aerosols in the air have the highest correlation (in most cases statistically significant) with the downward longwave radiation in the middle temperature interval. Downward longwave radiation is affected more by coarser aerosols and this conclusion is confirmed to some extent (the interval with the highest air temperatures) by the type of relationship between the downward longwave radiation and the Angstrom parameters, which is inversely proportional. Higher Angstrom parameter values are associated with smaller particle sizes and vice versa. In the case of a negative correlation coefficient, this means that finer aerosols are associated with less downward longwave radiation and vice versa. This robust relationship between coarser aerosol particles and longwave radiation causes most of the studies in this field to focus on

Table 3. Spearman's correlation coefficients between downward longwave radiation and the other studied variables for the different air temperature intervals during the period 01/2017 – 09/2019 at Musala peak. Statistically significant coefficients are bolded.

Variable	Downward longwave radiation – cases with air temperature below –5.5°C	Downward longwave radiation – cases with air temperature between –5.5°C and +5.5°C	Downward longwave radiation – cases with air temperature above 5.5°C
Specific humidity	0.57	0.71	0.48
AOT ₁₀₂₀	-0.05	0.40	0.11
AOT ₅₅₀	-0.09	0.38	0.11
SMPS _{totalsum}	-0.08	0.27	0.24
SMPS _{sum>285}	-0.17	0.35	0.33
Angstrom parameter ₄₇₀₋₈₇₀	0.20	-0.10	-0.38
Absorption _{blue}	0.02	0.25	-0.03
Absorption _{green}	0.07	0.23	-0.06
Absorption _{red}	0.20	0.30	0.02
Scattering _{blue}	-0.13	0.37	0.35
Scattering _{green}	-0.04	0.35	0.38
Scattering _{red}	-0.10	0.39	0.36
α Blue-Red scattering coefficient	0.15	0.06	-0.08
β Blue-Red scattering coefficient	0.00	0.33	0.33

dust or dust storms, as these conditions are characterized by a large size of aerosol particles. This type of aerosols (dust) predominates in the area of Musala peak only at high air temperatures and the corresponding relationship is statistically significant only in the third column of Table 3. During the cold part of the year this relationship even reverses its sign. This is due to the fact that during that part of the year the largest particles are snow or ice, and the smaller ones are possibly dust. This means that transparent aerosols have little or no effect on downward longwave radiation, unlike opaque ones. Whenever there is a lot of dust in the air, it is able to absorb some of the shortwave radiation, to heat, and then to emit longwave radiation towards the Earth's surface (Maghrabi and Al-Dosari, 2016; Antón et al., 2014; Slingo et al., 2006; Panicker et al., 2008). Due to this effect, the series of data of the absorption of radiation from aerosols at the three wavelengths in the visible spectrum were included in the present study. The results in Table 3 show that there is no significant relationship between the absorption of radiation from aerosols and downward longwave radiation. Thus, at Musala peak, this mechanism is not important – due to the relatively small amount of opaque aerosol particles. Aerosol scattering is in a positive and statistically significant relationship with the downward longwave radiation in the two intervals with air temperatures above –5.5°C. This relationship is due to the fact that scattering is largely related to the total amount of aerosols in the air. The results in Table 3 show that not only the amount of aerosols, but also their type and size, are important for their influence on downward longwave radiation. If only the opaque aerosols are considered, their higher amount and larger size lead to a stronger influence (positive relationship) on downward longwave radiation. However, the environmental conditions at Musala peak are more specific. There are two opposite tendencies in terms of the

influence of aerosols on downward longwave radiation, which depend on air temperature – as the air temperature increases, the amount of aerosols in the air increases, which enhances the positive correlation with the downward longwave radiation. On the other hand, as the air temperature increases, the size of aerosol particles decreases, which weakens the positive correlation with the downward longwave radiation. The type of aerosols also changes from transparent to opaque. That is why, the strongest relationship between the amount of aerosols in the air and the downward longwave radiation occurs in the middle temperature interval.

Linear and S-curve regression models were used to quantify the effect of the independent variables (specific humidity, AOT₁₀₂₀, AOT₅₅₀, total sum, sum>285 nm, etc.) on the dependent variable (downward longwave radiation). The results of the models are presented in Table 4 (air temperatures below –5.5°C), Table 5 (air temperatures between –5.5°C and +5.5°C), Table 6 (air temperatures above 5.5°C), and Fig. 7-11. The second column in Tables 4, 5 and 6 shows the type of model, the third column is the coefficient of determination (R^2), the fourth column is the significance of the model, and the fifth column is the value of b (linear model) or d (S-curve model). The sixth column of Table 5 shows the mean value of the independent variable (x_m), which is required for the calculations of the S-curve regression model. The percentage change (B) in the dependent variable when the independent variable changes by one unit, is shown in the sixth column of Tables 4 and 6, and the seventh column of Table 5. The values of B for the two types of models are calculated as follows:

Linear model. Its equation is:

$$y = a + b * x \quad (6)$$

The difference when changing the independent variable (x) by 1 unit, leads to the following equation:

$$y_2 - y_1 = a + b * (x + 1) - (a + b * x) \quad (7)$$

where y_2 is the value of the dependent variable when the independent variable is $x + 1$, and y_1 is the value of the dependent variable when the independent variable is x . Solving this equation gets:

$$y_2 = y_1 + b \quad (8)$$

B is calculated using the following formula:

$$B = \frac{b}{y_m} * 100 \quad (9)$$

where y_m is the mean of the dependent variable (downward longwave radiation); in the case of Musala peak it is $168.5 \text{ W} * \text{m}^{-2}$ for the air temperature interval below -5.5°C , $199.8 \text{ W} * \text{m}^{-2}$ for the air temperature interval between -5.5°C and $+5.5^\circ\text{C}$, and $241 \text{ W} * \text{m}^{-2}$ for the air temperature interval above 5.5°C .

S-curve model. Its equation can also be written as follows:

$$\ln y = c + \frac{d}{x} \quad (10)$$

The difference when changing the independent variable (x) by 1 unit, leads to the following equation:

$$\ln y_2 - \ln y_1 = \left(c + \frac{d}{x+1}\right) - \left(c + \frac{d}{x}\right) \quad (11)$$

where y_2 is the value of the dependent variable when the independent variable is $x + 1$, and y_1 is the value of the dependent variable when the independent variable is x . Solving this equation gets:

$$y_2 = y_1 * e^{-\left(\frac{d}{x^2+x}\right)} \quad (12)$$

The value of the independent variable x_m , which is the mean value shown in the sixth column of Table 5, is also used here, when calculating the value of B . This means that the calculated percentages of change will refer specifically to that mean value, which is typical for Musala peak. Here B is calculated using the following formula:

$$B = \left(e^{-\left(\frac{d}{x_m^2+x_m}\right)} - 1\right) * 100 \quad (13)$$

Because the units of measurement of the different independent variables differ significantly, in order to have comparability of the results, the last column of Tables 4, 5 and 6, shows the percentage change of the dependent variable when the independent variable changes by 1%. The calculation is done according to the following formula:

$$B_p = B * x_m \quad (14)$$

where B_p is the percentage change in the dependent variable per 1% change in the independent variable.

In accordance with the results in Table 3, the models with the highest values of the coefficient of determination and the lowest level of significance (Tables 4, 5 and 6), are the models describing the relationship between the specific humidity and the downward longwave radiation for all air temperature intervals. Accordingly, the percentage change in the dependent variable is highest, reaching values of about 11.5% (air temperatures below -5.5°C),

15.3% (air temperatures between -5.5°C and $+5.5^\circ\text{C}$) and 12.6% (air temperatures above 5.5°C) per 1% change in the independent variable. All previous studies which investigate in some form the water vapor parameter in the atmosphere, indicate it as a leading factor in determining the amount of downward longwave radiation. A quantitative assessment of this relationship (8%) is given only in the paper by Maghrabi et al. (2019). However, in their calculations the authors use an atmospheric radiative transfer model and precipitable water vapor, rather than specific humidity. The influence which the various parameters measuring the amount of aerosols in the air have on the downward longwave radiation is less than that of the specific humidity, as evidenced by the coefficients of determination. At air temperatures above -5.5°C , the scattering at all three measured wavelengths has a significant influence, as well as the turbidity coefficient calculated on the basis of the scattering in the blue and in the red spectra. In general, these parameters indicate the amount of aerosols in the area of Musala peak. If the independent variable is increased by 1%, the downward longwave radiation increases by about 3-4% in the case where scattering coefficients are the independent variable, and by about 2% in the case where turbidity coefficient is the independent variable. These percentages are lower than the percentage increase of downward longwave radiation observed in the case where specific humidity is the independent variable, but the models have a significance of less than 0.05, which means that these factors should be taken into account. This also shows the particular importance of measuring the amount of aerosols *in situ*. The amount of aerosols in the entire air column above Musala peak only affects the downward longwave radiation when air temperatures are between -5.5°C and $+5.5^\circ\text{C}$. The optical thickness of aerosols measured at a wavelength of 1020 nm shows stronger relationship with the downward longwave radiation compared to the optical thickness of aerosols measured at a wavelength of 550 nm, which once again proves that coarser aerosol particles have stronger influence. This is also confirmed by the statistically significant inversely proportional relationship between the Angstrom exponent and the downward longwave radiation at air temperatures above 5.5°C . There is a large difference between the percentages of change of the dependent variable when AOT_{1020} and AOT_{550} change by 1 %, which does not allow for an accurate estimate. The percentages based on scattering and turbidity coefficients are probably more accurate for the area of Musala peak. Also, at air temperatures above 5.5°C , the increase of the Angstrom exponent by 1% (finer particles) leads to a decrease of the downward longwave radiation by about 8% and vice versa. It should be emphasized once again that all calculations refer to the region of Musala peak, which has specific environmental conditions. In other environmental conditions, the results could be different.

Table 4. Type of best fitting model (equation), R^2 , significance (p), coefficient b , percentage change in the dependent variable (downward longwave radiation) (B in %) per unit change in the independent variable, and percentage change (B_p in %) in the dependent variable (downward longwave radiation) per 1% change in the independent variable, for cases with air temperature below -5.5°C during the period 01/2017 – 09/2019 at Musala peak.

Independent variable	Equation	R^2	Significance	b	B	B_p
Specific humidity	Linear	0.23	0.001966	10525.34	6245.63	11.51

Table 5. Type of best fitting model (equation), R^2 , significance (p), coefficient b (linear models) or d (S-curve model), mean value of the independent variable (x_m), percentage change in the dependent variable (downward longwave radiation) (B in %) per unit change in the independent variable, and percentage change (B_p in %) in the dependent variable (downward longwave radiation) per 1% change in the independent variable, for the different independent variables, for cases with air temperature between -5.5°C and $+5.5^\circ\text{C}$ during the period 01/2017 – 09/2019 at Musala peak.

Independent variable	Equation	R^2	Significance	b/d	x_m	B	B_p
Specific humidity	Linear	0.48	0	11373.19		5692.72	15.29
AOT ₁₀₂₀	Linear	0.30	0.000038	123.6406		61.89	9.56
AOT ₅₅₀	S-curve	0.15	0.00354	-0.0057	0.084274	6.44	0.54
Scattering _{blue}	Linear	0.18	0.002827	105218.4		52665.84	4.11
Scattering _{green}	Linear	0.17	0.003339	126215.9		63175.91	3.42
Scattering _{red}	Linear	0.15	0.006636	136034.6		68090.54	2.74
β Blue-Red scattering coefficient	Linear	0.10	0.038083	116935.4		58530.63	1.68

Table 6. Type of best fitting model (equation), R^2 , significance (p), coefficient b , percentage change in the dependent variable (downward longwave radiation) (B in %) per unit change in the independent variable, and percentage change (B_p in %) in the dependent variable (downward longwave radiation) per 1% change in the independent variable, for the different independent variables, for cases with air temperature above 5.5°C during the period 01/2017 – 09/2019 at Musala peak.

Independent variable	Equation	R^2	Significance	b	B	B_p
Specific humidity	Linear	0.29	0.000228	6043.612	2507.78	12.55
Angstrom parameter ₄₇₀₋₈₇₀	Linear	0.10	0.04729	-15.1556	-6.29	-8.42
Scattering _{blue}	Linear	0.17	0.008302	72384.29	30035.67	4.32
Scattering _{green}	Linear	0.18	0.005099	107988.9	44809.69	4.51
Scattering _{red}	Linear	0.18	0.005192	133597.3	55435.85	3.87
β Blue-Red scattering coefficient	Linear	0.16	0.010358	152983.7	63480.18	2.66

Figure 7. Scatter plot of the values of downward longwave radiation ($\text{W}\cdot\text{m}^{-2}$) against the values of specific humidity ($\text{kg}\cdot\text{kg}^{-1}$) for the selected cases with air temperatures between -5.5°C and $+5.5^\circ\text{C}$ during the period 01/2017 – 09/2019 at Musala peak. The best fitting model is a linear model.

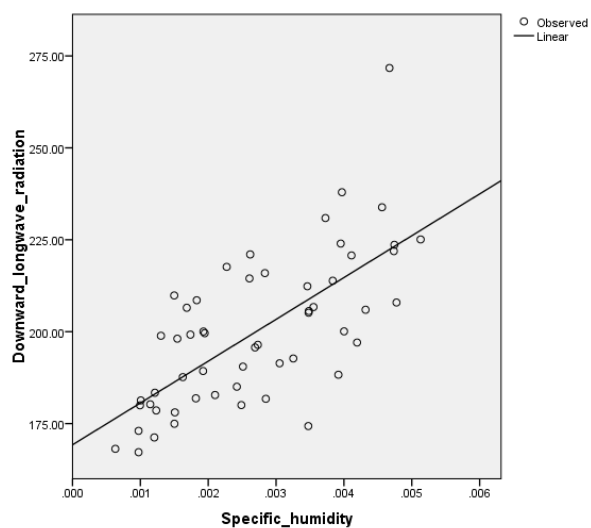


Figure 8. Scatter plot of the values of downward longwave radiation ($\text{W}\cdot\text{m}^{-2}$) against the values of AOT₁₀₂₀ for the selected cases with air temperatures between -5.5°C and $+5.5^\circ\text{C}$ during the period 01/2017 – 09/2019 at Musala peak. The best fitting model is a linear model.

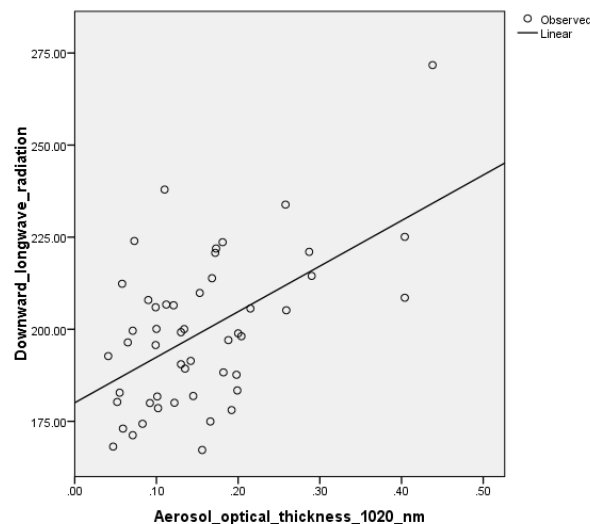


Figure 9. Scatter plot of the values of downward longwave radiation ($W \cdot m^{-2}$) against the values of AOT_{550} for the selected cases with air temperatures between $-5.5^{\circ}C$ and $+5.5^{\circ}C$ during the period 01/2017 – 09/2019 at Musala peak. The best fitting model is the S-curve model.

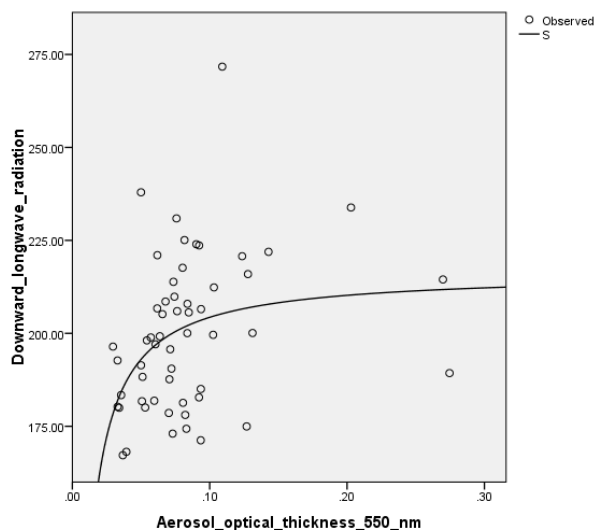


Figure 11. Scatter plot of the values of downward longwave radiation ($W \cdot m^{-2}$) against the values of the turbidity coefficient β (blue-red scattering) for the selected cases with air temperatures between $-5.5^{\circ}C$ and $+5.5^{\circ}C$ during the period 01/2017 – 09/2019 at Musala peak. The best fitting model is a linear model.

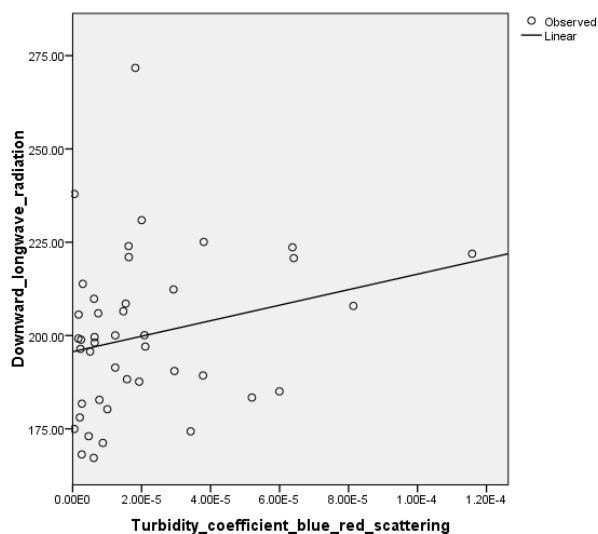
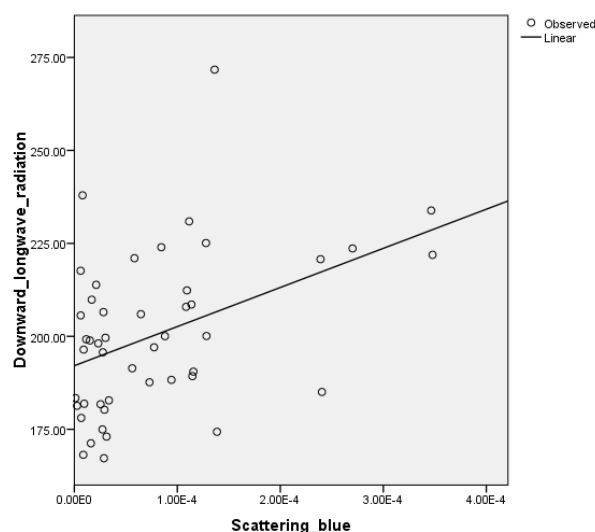


Figure 10. Scatter plot of the values of downward longwave radiation ($W \cdot m^{-2}$) against the values of $Scattering_{blue}$ ($M \cdot m^{-1}$) for the selected cases with air temperatures between $-5.5^{\circ}C$ and $+5.5^{\circ}C$ during the period 01/2017–09/2019 at Musala peak. The best fitting model is a linear model.



4. Conclusion

The results presented in this study indicate that air temperature has a significant influence on the downward longwave radiation, the specific humidity and the amount of aerosols in the air in the region of Musala peak. And while for the first two elements this is logical, based on their specificity, as far as the amount of aerosols is concerned, the dependence is not so obvious but can be explained by the more active movements in the atmosphere and the lack of snow cover at higher air temperatures. Accordingly, if it is necessary to find the pure relationship between downward longwave radiation, specific humidity and amount of aerosols in the atmosphere, this factor (air temperature) should be cleared from the data series. After removing the air temperature factor, the results show that specific humidity has a big influence on the downward longwave radiation flux, and a change by 1% in the values of specific humidity results in a change by about 12-15% in the values of downward longwave radiation. This relationship is directly proportional, which means that the higher content of water vapor in the atmosphere leads to a higher flux of downward longwave radiation and vice versa. It should also be noted that at air temperatures around $0^{\circ}C$ the influence of water vapor on the downward longwave flux is highest, which is due to the phase transitions of the water, which release/absorb radiation in the longwave spectrum. Atmospheric aerosols also exert a significant influence on downward longwave radiation, mainly when air temperatures are above $-5.5^{\circ}C$. Several characteristics of aerosols determine their influence – their amount in the air, their size and their type (transparent/opaque). The results of the study show that the higher amount of aerosols in the air leads to a more significant effect on the increase of the downward longwave radiation flux. Coarser aerosol particles have a stronger effect on downward longwave radiation. Also, opaque aerosol particles have a stronger effect on downward longwave radiation. In the area of Musala peak, as the air temperature rises, there is an increase of the amount of aerosols in the air, a decrease in their size and a transition from transparent to opaque aerosols. The combination of these

different tendencies leads to the fact that the influence of aerosols on the downward longwave radiation is strongest in the middle temperature interval – air temperatures between -5.5°C and $+5.5^{\circ}\text{C}$. Due to the increased total amount of aerosols and the increased amount of opaque aerosols, their influence on downward longwave radiation is significant also at air temperatures above 5.5°C . In these two temperature intervals, the measurements of the aerosol amount in the area of Musala peak show a better connection with downward longwave radiation compared to the measurements of the aerosol amount in the entire air column above the peak. It can be concluded that an increase by 1% of the amount of aerosols in the near-surface air leads to an increase by about 2 to 4% of the downward longwave radiation at air temperatures above -5.5°C .

Acknowledgments

This study was supported by Aerosols, clouds and trace gases infrastructure implementation project (ACTRIS IMP), EU Horizon 2020 coordination and support action, grant agreement No 871115.

Author contributions

Peter Nojarov: Conceptualization, Methodology, Formal analysis, Investigation, Writing - Original Draft, Writing - Review and Editing, Visualization; Todor Arsov: Software, Validation, Data Curation; Ivo Kalapov: Validation, Resources, Data Curation; Hristo Angelov: Resources, Supervision, Project administration, Funding acquisition.

Declaration

The authors have declared that no competing interests exist.

References

- Angstrom A (1918) A study of the radiation of the atmosphere. Smithsonian Institution Miscellaneous Collections 65: 159–161.
- Angstrom A (1964) The parameters of atmospheric turbidity. *Tellus* 16, 64–75.
- Antón M, Valenzuela A, Mateos D, Alados I, Foyo-Moreno I, Olmo FJ, Alados-Arboledas L (2014) Longwave aerosol radiative effects during an extreme desert dust event in southeastern Spain. *Atmospheric research* 149: 18–23. <http://dx.doi.org/10.1016/j.atmosres.2014.05.022>
- Asmi A, Wiedensohler A, Laj P, Fjaeraa A-M, Sellegri K, Birmili W, Weingartner E, Baltensperger U, Zdimal V, Zikova N, Putaud J-P, Marinoni A, Tunved P, Hansson H-C, Fiebig M, Kivekas N, Lihavainen H, Asmi E, Ulevicius V, Aalto PP, Swietlicki E, Kristensson A, Mihalopoulos N, Kalivitis N, Kalapov I, Kiss G, de Leeuw G, Henzing B, Harrison RM, Beddows D, O'Dowd C, Jennings SG, Flentje H, Weinhold K, Meinhardt F, Ries L, Kulmala M (2011) Number size distributions and seasonality of submicron particles in Europe 2008–2009. *Atmospheric Chemistry and Physics* 11: 5505–5538. <https://doi.org/10.5194/acp-11-5505-2011>
- Barragan R, Romano S, Sicard M, Burlizzi P, Perrone MR, Comeron A (2016) Estimation of mineral dust direct radiative forcing at the European Aerosol Research Lidar NETwork site of Lecce, Italy, during the ChArMEX/ADRIMED summer 2013 campaign: Impact of radiative transfer model spectral resolutions. *Journal of Geophysical Research: Atmospheres* 121 (17): 10–237. <https://doi.org/10.1002/2016JD025016>
- Brunt D (1932) Notes on radiation in the atmosphere. *Quarterly Journal of the Royal Meteorological Society* 58: 389–418.
- Brutsaert W (1975) On a derivable formula for long-wave radiation from clear skies. *Water Resources Research* 11: 742–744.
- Del Guasta M, Marini S (2000) On the retrieval of urban aerosol mass concentration by a 532 and 1064 nm LIDAR. *Journal of Aerosol Science* 31 (12): 1469–1488. [https://doi.org/10.1016/S0021-8502\(00\)00049-5](https://doi.org/10.1016/S0021-8502(00)00049-5)
- Del Guasta M (2002) Daily cycles in urban aerosols observed in Florence (Italy) by means of an automatic 532–1064 nm LIDAR. *Atmospheric Environment* 36: 2853–2865. [https://doi.org/10.1016/S1352-2310\(02\)00136-X](https://doi.org/10.1016/S1352-2310(02)00136-X)
- Donev E (1983) Measurement methods in meteorology. Printing house of Sofia University “St. Kl. Ohridski”, Sofia, 380 pp. (in Bulgarian)
- Dufresne JL, Gautier C, Ricchiazzi P, Fouquart Y (2002) Longwave scattering effects of mineral aerosols. *Journal of the Atmospheric Sciences* 59 (12): 1959–1966. [https://doi.org/10.1175/1520-0469\(2002\)059<1959:LSEO MA>2.0.CO;2](https://doi.org/10.1175/1520-0469(2002)059<1959:LSEO MA>2.0.CO;2)
- Gelaro R, McCarty W, Suárez MJ, Todling R, Molod A, Takacs L, Randles CA, Darmenov A, Bosilovich MG, Reichle R, Wargan K, Coy L, Cullather R, Draper C, Akella S, Buchard V, Conaty A, da Silva AM, Gu W, Kim G, Koster R, Lucchesi R, Merkova D, Nielsen JE, Partyka G, Pawson S, Putman W, Rienecker M, Schubert SD, Sienkiewicz M, Zhao B (2017) The Modern-Era Retrospective Analysis for Research and Applications, Version 2 (MERRA-2). *Journal of Climate* 30: 5419–5454. <https://doi.org/10.1175/JCLI-D-16-0758.1>
- Idso SB, Jackson RD (1969) Thermal radiation from the atmosphere. *Journal of Geophysical Research* 74: 5397–5403.
- Maghrabi AH, Al-Dosari AF (2016) Effects on surface meteorological parameters and radiation levels of a heavy dust storm occurred in Central Arabian Peninsula. *Atmospheric Research* 182: 30–35. <http://dx.doi.org/10.1016/j.atmosres.2016.07.024>
- Maghrabi AH, Almutayri MM, Aldosary AF, Allehyani BI, Aldakhil AA, Aljarba GA, Alttilasi MI (2019) The influence of atmospheric water content, temperature, and aerosol optical depth on downward longwave radiation in arid conditions. *Theoretical and Applied Climatology* 138 (3–4): 1375–1394. <https://doi.org/10.1007/s00704-019-02903-y>
- Nojarov P, Kalapov I, Stamenov J, Arsov T (2014) Some connections between aerosols, atmospheric transport, and relative humidity at peak Musala. *Theoretical and Applied Climatology* 115 (3–4): 471–482. <https://doi.org/10.1007/s00704-013-0906-0>
- Nojarov P (2017) Influence of composition of atmosphere over Bulgaria on surface radiation fluxes and air temperature. *Problems of Geography* 4: 57–78. <https://doi.org/10.35101/PRG-2017.4.5>
- Nojarov P, Arsov T, Kalapov I, Angelov H (2021) Aerosol direct effects on global solar shortwave irradiance at high mountainous station Musala, Bulgaria. *Atmospheric Environment*, 244: 117944. <https://doi.org/10.1016/j.atmosenv.2020.117944>
- Panicker AS, Pandithurai G, Safai PD, Kewat S (2008) Observations of enhanced aerosol longwave radiative forcing over an urban environment. *Geophysical Research Letters* 35: L04817. <https://doi.org/10.1029/2007GL032879>
- Prata AJ (1996) A new long-wave formula for estimating downward clear-sky radiations at the surface. *Quarterly Journal of the Royal Meteorological Society* 122: 1127–1151.
- Slingo A, Ackerman TP, Allan RP, Kassianov EI, McFarlane SA, Robinson GJ, Barnard JC, Miller MA, Harries JE, Russell JE, Dewitte S (2006) Observations of the impact of a major Saharan dust storm on the atmospheric radiation balance. *Geophysical Research Letters* 33 (24): L24817. <https://doi.org/10.1029/2006GL027869>
- Song Q, Zhang Z, Yu H, Seiji K, Yang P, Colarco P, Remer L, Ryder C (2018) Net radiative effects of dust in the tropical North Atlantic based on integrated satellite observations and in situ measurements. *Atmospheric Chemistry and Physics* 18: 11303–11322. <https://doi.org/10.5194/acp-18-11303-2018>
- Swinbank WC (1963) Long-wave radiation from clear skies. *Quarterly Journal of the Royal Meteorological Society* 89: 339–348.
- Venzac H, Sellegri K, Villani P, Picard D, Laj P (2009) Seasonal variation of aerosol size distributions in the free troposphere and residual layer at

- the puy de Dôme station, France. *Atmospheric Chemistry and Physics* 9: 1465–1478. <https://doi.org/10.5194/acp-9-1465-2009>
- Wang C, Tang BH, Wu H, Tang R, Li ZL (2017) Estimation of Downwelling Surface Longwave Radiation under Heavy Dust Aerosol Sky. *Remote Sensing* 9 (3): 207. <https://doi.org/10.3390/rs9030207>
- Wang H, Shi G, Teruo A, Wang B, Zhao T (2004) Radiative forcing due to dust aerosol over east Asia-north Pacific region during spring, 2001. *Chinese Science Bulletin* 49 (20): 2212-2219. <https://doi.org/10.1007/BF03185790>
- Weingartner E, Nyeki S, Baltensperger U (1999) Seasonal and diurnal variation of aerosol size distributions ($10 < D < 750$ nm) at a high-alpine site (Jungfraujoch 3580 m asl). *Journal of Geophysical Research: Atmospheres* (1984–2012) 104 (D21): 26809-26820. <https://doi.org/10.1029/1999JD900170>
- Wilks DS (2006) *Statistical Methods in the Atmospheric Sciences*. Volume 91. Second Edition (International Geophysics), Elsevier.

ORCID

- <https://orcid.org/0000-0002-9635-2304> - P. Nojarov
<https://orcid.org/0000-0002-2537-5058> - T. Arsov
<https://orcid.org/0000-0001-9515-1343> - I. Kalapov
<https://orcid.org/0000-0002-2562-8924> - H. Angelov